Pharmacological Research 192 (2023) 106794

Contents lists available at ScienceDirect

Pharmacological Research

journal homepage: www.elsevier.com/locate/yphrs

A multi-omics investigation of tacrolimus off-target effects on a proximal tubule cell-line

Hassan Aouad [a], Quentin Faucher [a], François-Ludovic Sauvage [a], Emilie Pinault [a], Claire-Cécile Barrot [a], Hélène Arnion [a], Marie Essig [a,b,1,2], Pierre Marquet [a,c,*,1]

[a] Pharmacology & Transplantation, Université de Limoges, INSERM U1248, Limoges, France
[b] Department of Nephrology, CHU Limoges, Limoges, France
[c] Department of Pharmacology, Toxicology and Pharmacovigilance, CHU Limoges, Limoges, France

ARTICLE INFO

Keywords:
Kidney
Transplantation
Tacrolimus
Toxicity
Mechanism
Omics

Chemical compounds studied in this article:
Tacrolimus (PubMed CID: 445643)

ABSTRACT

Introduction: Tacrolimus, an immunosuppressive drug prescribed to a majority of organ transplant recipients is nephrotoxic, through still unclear mechanisms. This study on a lineage of proximal tubular cells using a multi-omics approach aims to detect off-target pathways modulated by tacrolimus that can explain its nephrotoxicity.
Methods: LLC-PK1 cells were exposed to 5 μM of tacrolimus for 24 h in order to saturate its therapeutic target FKBP12 and other high-affine FKBPs and favour its binding to less affine targets. Intracellular proteins and metabolites, and extracellular metabolites were extracted and analysed by LC-MS/MS. The transcriptional expression of the dysregulated proteins PCK-1, as well as of the other gluconeogenesis-limiting enzymes FBP1 and FBP2, was measured using RT-qPCR. Cell viability with this concentration of tacrolimus was further checked until 72 h.
Results: In our cell model of acute exposure to a high concentration of tacrolimus, different metabolic pathways were impacted including those of arginine (e.g., citrulline, ornithine) ($p < 0.0001$), amino acids (e.g., valine, isoleucine, aspartic acid) ($p < 0.0001$) and pyrimidine ($p < 0.01$). In addition, it induced oxidative stress ($p < 0.01$) as shown by a decrease in total cell glutathione quantity. It impacted cell energy through an increase in Krebs cycle intermediates (e.g., citrate, aconitate, fumarate) ($p < 0.01$) and down-regulation of PCK-1 ($p < 0.05$) and FPB1 ($p < 0.01$), which are key enzymes in gluconeogenesis and acid-base balance control.
Discussion: The variations found using a multi-omics pharmacological approach clearly point towards a dysregulation of energy production and decreased gluconeogenesis, a hallmark of chronic kidney disease which may also be an important toxicity pathway of tacrolimus.

1. Introduction

Tacrolimus is an immunosuppressive drug widely used to prevent graft rejection after solid organ transplantation and to treat autoimmune diseases [6]. Its whole blood concentrations should be within a narrow therapeutic range of 4–15 ng/ml to avoid underexposure and increased risks of rejection, and overexposure known to entail acute and chronic nephrotoxicity. Acute nephrotoxicity, linked to tacrolimus blood level > 20 ng/ml, is caused by hemodynamic perturbations and is reversible [5]. In contrast, chronic nephrotoxicity is an irreversible decline of renal function that can appear along time even in patients exposed to (low) pharmacological levels of tacrolimus.

The mechanism of tacrolimus nephrotoxicity is still not fully understood. Many studies were conducted on proximal tubular cells and

Abbreviations: PCK-1, phosphoenolpyruvate carboxykinase 1; FBP1, Fructose biphosphatase 1; FBP2, Fructose biphosphatase 2; LLC-PK1, Lilly Laboratories Cells Porcine Kidney 1; LC-MS/MS, liquid chromatography coupled to tandem mass spectrometry; MTS, 3-(4,5-dimethylthiazol-2-yl)− 5-(3-carboxymethoxyphenyl)− 2-(4-sulfophenyl)− 2 H-tetrazolium; NADPH, Nicotinamide adenine dinucleotide phosphate; PCA, Principal component analysis.

* Correspondence to: Service de Pharmacologie, Toxicologie et Pharmacovigilance, Centre Hospitalier Universitaire de Limoges, CBRS, 2 rue Bernard Descottes, 87000 Limoges, France.
E-mail address: pierre.marquet@unilim.fr (P. Marquet).
[1] These authors contributed equally to this work and share last authorship
[2] Present address: Department of Nephrology, Ambroise Paré Hospital, APHP, Paris Saclay University, Boulogne Billancourt, France

https://doi.org/10.1016/j.phrs.2023.106794
Received 14 February 2023; Received in revised form 8 May 2023; Accepted 12 May 2023
Available online 13 May 2023

linked nephrotoxicity either to a mitochondrial toxicity characterized by functional and structural perturbation of the mitochondria [18,29], or to increased oxidative stress caused by an increase of intracellular H_2O_2 levels or a decrease in MnSOD, an antioxidant enzyme [17,32]. Autophagy was also found to be disrupted in cells exposed to tacrolimus, with an accumulation of autophagy vesicles in the cytoplasm [19,31]. Furthermore, cells exposed to tacrolimus were also reported to lose some transporter-related functions [24].

To explore further tacrolimus off-target effects that might point towards pathways involved in its toxicity on the proximal tubule, we designed this multi-omics study to screen for intracellular and extracellular modifications of LLC-PK1 cells incubated with a high concentration of tacrolimus over a short period of time, so as to saturate its therapeutic target FKBP12 and other high-affine FKBPs and favour its binding to less affine targets. We confirmed that tacrolimus induces an oxidative stress and found that it also affects the arginine and energetic metabolisms, as suggested by increased quantities of intermediates of the citric acid cycle and down-regulation of PCK-1 and FBP1, which are gluconeogenesis-limiting enzymes. In addition, tacrolimus modified the metabolism of purine bases.

2. Materials and methods

2.1. Chemicals and reagents

Dulbecco's Modified Eagle's Medium (DMEM)-Ham's F12 (1:1, 31331), Fetal Bovine Serum (10500), 1 M HEPES (15630), 7.5% Sodium bicarbonate (25080), 10,000 UI/ml Penicillin/ Streptomycin (15140), Dulbecco's Phosphate Buffer Saline (14190), Superscript II RT (180064022, Invitrogen™) were purchased from ThermoFisher Scientific (Illkrich-Graffenstaden, France). Sodium selenite (S5261), insulin (I4011), triiodothyronine (T6397), dexamethasone (D4902), human apo-transferrin (T1147), desmopressin (V1005), tacrolimus (F4679), 2-isopropylmalic acid (333115), DTT (1.4-Dithiothritol) (D0632), Urea (U5378), Iodoacetamide (I1149), AmiconUltra-0.5 centrifugal filters (UFC5010), DNase I Kits (AMPD1) and 2-D Quant KIT (GE80–6483–56, Cytiva™) were purchased from Sigma-Aldrich (St. Quentin Fallavier, France). NuleoSpin® RNA/Protein extraction kits (740933.50) were purchased from Macherey-Nagel (Hoerdt, France). Sequencing grade modified trypsin (V5111), RNasin® ribonuclease inhibitor (N2511), random primers (C118A) and MTS (G3581) were obtained from Promega (Courtaboeuf, France). QuantiFast® SYBER® Green PCR Kits (204054) were purchased from Qiagen. HLB oasis 3cc 60 mg cartridges (WAT094226) were obtained from Water (saint Quentin en Yvelines, France).

2.2. Cell culture conditions

LLC-PK1 (Lilly Laboratories Porcine Kidney-1) porcine proximal tubule cells (ATCC-CL-101, ATCC, Manassas, VA) were expanded in 75 cm^2 flasks at 37 °C with 5% CO_2 and passed once confluence was reached. The culture medium consisted in a 1:1 DMEM-Ham's F12 mix supplemented with 5% FBS, 15 mM HEPES, 0.1% Sodium bicarbonate, 100 UI/ml Penicillin / Streptomycin and 50 nM Sodium selenite. LLC-PK1 cells were cultured between passage 7 and passage 20.

They were seeded in 6-well plates and expanded up to subconfluence in the routine cell culture medium. Seeded LLC-PK1 sustained serum starvation and were fed with hormonally defined (25 μg/ml insulin, 11 μg/ml transferrin, 50 nM triiodothyronine, 0.1 μM dexamethasone, 0.1 μg/ml desmopressin) fresh medium to engage epithelial differentiation, for 24 h. After differentiation, two treatment conditions were applied for 24 h: i) ethanol 0.5% (control); or ii) tacrolimus 5 μM in 0.5% ethanol. For intracellular and extracellular metabolomics investigations, 3 and 4 independent experiments were performed in triplicate, respectively. For the proteomics study, 6 independent experiments were performed in singlicate.

2.3. Viability test

To check that the high tacrolimus concentration chosen would not have induced cell mortality shortly after the time chosen for multi-omics investigations (24 h), LLCPK1 were incubated with 5 μM tacrolimus for 72 h.

For this, cells were seeded in 96-well plates at 25,000 cells/well for 24 h, then differentiated for 24 h and treated with either 0.5% ethanol (control) or 5 μM tacrolimus. Culture medium, with and without tacrolimus, was changed every 24 h for 72 h. Viability was assessed using the MTS test according to the manufacturer's instruction. Measurement of the absorbance was performed on PerkinElmer EnSpire® Multimode Plate Reader.

Viability was also assessed using flow cytometry. Briefly, cells were cultured in 6-well plates at 500,000 cells/well, incubated with 5 μM tacrolimus for 72 h as described above, washed twice with PBS and detached with trypsin EDTA. Detached cells were then washed twice with PBS and stained with annexin 5/7AAD. Reading was performed on a BD LSRFortessa™ flow cytometer.

2.4. Metabolomics study

2.4.1. Sample preparation

Extraction of intracellular metabolites was based on a previously published method [30]. Treated and control cells were washed twice with ice cold PBS and then lysed using 3 ml of a mixture of methanol/water 80%/20% volume spiked with 2-isopropylmalic acid at a final concentration of 500 nM (internal standard) and incubated for 20 min at − 80 °C. Every well was then scrapped using cell scrapper, cell lysates transferred to 5 ml Eppendorf tubes and centrifuged at 20,000 g for 5 min at 4 °C. One milliliter of each supernatant was then transferred into a 1.5 ml Eppendorf tube and evaporated to dryness in a vacuum concentrator. The extract was then solubilized with 50 μL of MiliQ water and transferred to a vial for mass spectrometry analysis.

Extracellular metabolites were extracted following manufacturer's instructions (Shimadzu). The culture medium of treated cells was collected and centrifuged at 3000 g for 1 min at room temperature to eliminate cell debris. Then, to 100 μL of the supernatant were added 200 μL of acetonitrile and 20 μL of internal standard (2-isopropylmalic acid [500 μM]). After homogenization, samples were centrifuged at room temperature for 15 min at 15,000 g. The supernatant was then diluted 1/10 in ultrapure water and transferred into an injection vial for mass spectrometry analysis.

2.4.2. Metabolomics LC-MS/MS analysis

Three μL of the suspended extracts were injected into the analytical system. Mass spectrometry analyses were performed using a LCMS-8060 (Shimadzu) tandem mass spectrometer and the LC-MS/MS "Method Package for Cell Culture Profiling Ver.2" (Shimadzu). The mass transitions of additional compounds were added after infusing the pure substances in the mass spectrometer. For each transition analyzed, only well-defined chromatographic peaks were considered. The area under the curve of each metabolite was normalized to the area under the curve of the internal standard (2-isopropylmalic acid).

2.4.3. Data analysis and statistics

In every experiment, treated samples were normalized by the corresponding control. MetaboAnalyst 5.0 computational platform (www.metaboanalyst.ca/faces/home.xhtml) was used for all statistical analyses. Univariable analysis was performed using the t-test; p-values were corrected for multiple testing using the False Discovery Rate (FDR) method. Multivariate exploration and unsupervised analysis by Principal Component Analyses (PCA) were performed.

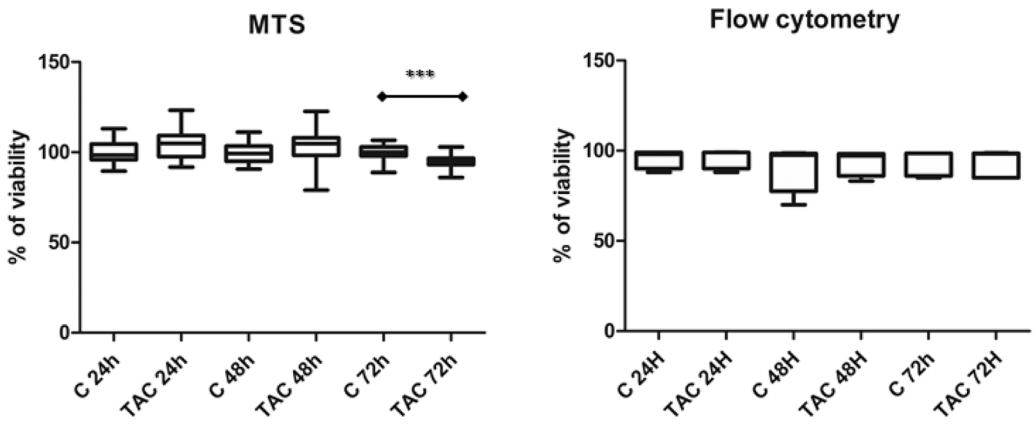

Fig. 1. Viability of the tubular proximal cell line exposed to tacrolimus. LLC-PK1 viability after incubation with 0.5% ethanol (control (C)) or 5 μM of tacrolimus in 0.5% ethanol (TAC) for 24 h, 48 h and 72 h, assessed using the MTS viability assay (n = 18, left graph) and annexin 5/ 7AAD staining (n = 5, right graph). Graphs represent the % of viable cells with tacrolimus as compared to control for each incubation duration. * ** $p < 0.001$ by Student t-test.

2.5. Proteomics study

2.5.1. Sample preparation

For intracellular proteomics, treated and control cells were washed twice with ice cold PBS and then extracted with the NucleoSpin® RNA/ Protein extraction kit following manufacturer's instructions. The extracts were then stored at − 80 °C until analysis.

For intracellular proteomics, protein content was estimated using the 2D Quant kit following manufacturer's instruction. Thereafter, 50 μg of proteins were diluted in q.s. 200 μL of 8 M urea followed by 20 μL of 50 mM DDT and the samples were then incubated at 56 °C for 20 min. Next, 20 μL of 100 mM iodoacetamide were added and the samples incubated in the dark for 20 min. The reduced samples were transferred to an Amicon ultra-centrifugal filter and centrifuged at 14,000 *g* for 15 min. After the first centrifugation, the samples were washed twice by 8 M urea and then twice with 25 mM ammonium bicarbonate. Digestion was performed on the filter by adding 10 μL of a solution of 0.1 μg/μL of trypsin and the mixture was incubated for 3 h at 37 °C. Peptides were recovered by centrifuging the Amicon filter at 14,000 *g* for 15 min, washing it with 100 μL of 1.5 M NaCl, putting it upside down in the tube and finally centrifuging at 1000 *g* for 2 min. Solid Phase Extraction (SPE) of the peptides was performed using OASIS® HLB cartridges (Waters) preconditioned with 3 ml of methanol and 3 ml of water/formic acid 0.5%. After loading, the diluted sample was first washed with 3 ml of water/formic acid 0.5% and then with 3 ml of water/methanol/formic acid (94.5/5/0.5, v/v/v). The cartridge was dried for 15 min and elution achieved with 3 ml of acetonitrile/water (70/30, v/v). The eluate was evaporated under nitrogen and the dry residue was dissolved in 100 μL of water/acetonitrile/trifluoracetic acid (TFA) (98/2/0.05, v/v/v). The sample was then filtered on a 0.22 μm spin filter (Agilent) and analyzed by mass spectrometry.

2.5.2. Proteomics MicroLC-MS/MS analysis

The peptides resulting from protein digestion were analyzed by microLC-MS/MS using a nanoLC 425 liquid chromatography system in the micro-flow mode (Eksigent, Dublin, CA), coupled to a quadrupole-time-of-flight tandem mass spectrometer (TripleTOF 5600 +, Sciex, Framingham, MA) operated in the high-sensitivity mode. Reverse-phase LC was performed in a trap-and-elute configuration using a trap column (C18 Pepmap100 cartridge, 300 μm i.d. x 5 mm, 5 μm; Thermo Scientific) and a C18 analytical column (ChromXP, 150 ×0.3 mm i.d., 120 Å, 3 μm; Sciex) with the following mobile phases: loading solvent (water/ acetonitrile/trifluoroacetic acid 98/2/0.05 (v/v)), solvent A (0.1% (v/v) formic acid in water) and solvent B (water/acetonitrile/formic acid 5/ 95/0.1% (v/v)). All samples were loaded, trapped and desalted using a loading solvent flowrate of 10 μL/min for 5 min. Chromatographic separation was performed at a flow rate of 3 μL/min as follows: initial, 5% B, increased to 25% in 145 min, then to 95% B in 10 min, maintained at 95% for 15 min, and finally, decreased to 5% B for re-equilibration.

One μg of each sample (equivalent protein content) was first subjected to data-dependent acquisition (DDA) to generate the SWATH-MS spectral library. MS and MS/MS data were continuously recorded with up to 30 precursors selected for fragmentation from each MS survey scan. Precursor selection was based upon ion intensity, whether or not the precursor had previously been selected for fragmentation (dynamic exclusion). Ions were fragmented using the rolling collision energy setting. All DDA mass spectrometry files were searched using ProteinPilot software v.5.0.1 (Sciex) and the Paragon algorithm. Data were analyzed using the following parameters: cysteine alkylation with iodoacetamide, digestion by trypsin and no special factors. The search was conducted using UniProt database (June 2018 release) containing non-redundant proteins of *Sus scrofa*. The output of this search was used as the reference spectral library.

For sample analysis, the equivalent of 1 μg protein content was injected in the analytical system and subjected to data-independent acquisition (DIA) using 60 variable swath windows over the 400–1250 *m/z* range. For these experiments, the mass spectrometer was operated in such a way that a 50-ms survey scan (TOF-MS) was acquired and subsequent MS/MS experiments were performed on all precursors using an accumulation time of 120 ms per swath window for a total cycle time of 7.3 s. Parent ions were fragmented using rolling collision energy adjusted to the *m/z* range window. DIA samples were processed using PeakView v.2.1 (Sciex) with SWATH v.2.0 module and the reference spectral library generated above. Spectral alignment and targeted data extraction were performed using an extraction window of 15 min and the following parameters: protein identity confidence > 99% with a maximum of 10 peptides per protein and 5 fragments per peptide with 10 ppm error tolerance. Shared and modified peptides were excluded.

2.5.3. Data analysis and statistics

Statistical analysis of proteomics results was performed using the following R packages: Outliers, preprocessCore, tidyverse, rstatix and BBmisc. First, each batch of treated and control cells was normalized classically (centered and scaled). Second, delta values were computed from normalized data, as follows:

For each protein i, $Delta_i = \ln\left(\frac{treated_i}{control_i}\right)$.

Third, proteins with delta <ln(0.8) or > -ln(0.8), reflecting a decrease or increase of protein expression by more than 20% and identified using more than 2 peptides, were regarded as differentially expressed.

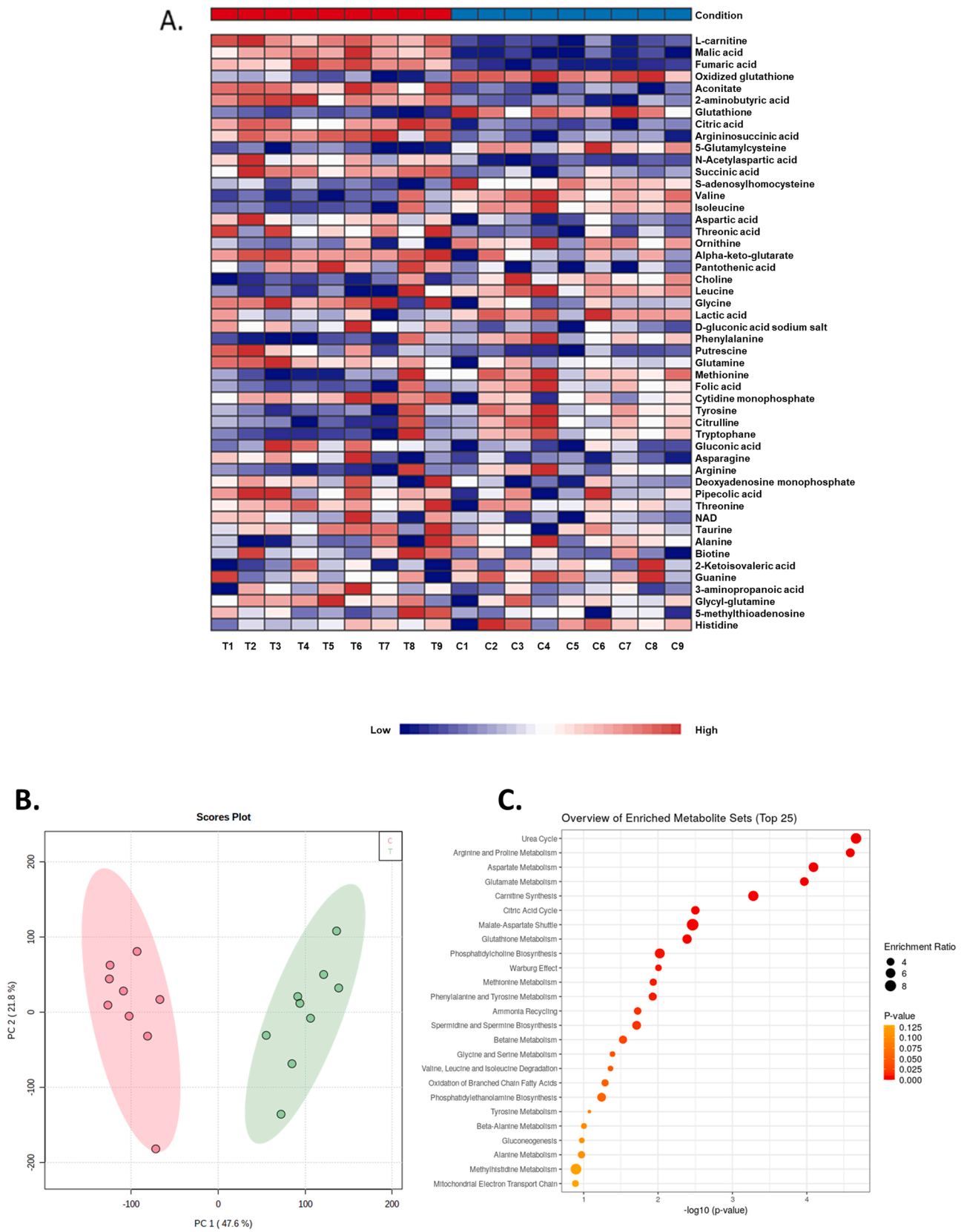

Fig. 2. Multivariate exploration of intracellular metabolites variations after 24 h tacrolimus exposure (n = 9). **A.** Heatmap clustering distinguishing the control condition (C) from tacrolimus-treated cells (T), based on all metabolites detected by LC-MS/MS. **B.** PCA scores plot showing complete separation between groups (C) and (T) with principal components PC1 and PC2 describing 47.6% and 21.8% of the variations, respectively (0 (red circles): 0.5% ethanol (control); 1 (green circles): tacrolimus 5 μM). **C.** Dot plot of pathway enrichment analysis based on the intracellular concentrations of metabolites significantly modified in tacrolimus-treated cells as compared to controls (Table 1).

Table 1
Fold-change of intracellular metabolites significantly influenced by tacrolimus (n = 9) (p-value<0.05).

Metabolite	Fold-change	P-value (T-test)	FDR
L-Carnitine	1.7425	8.9464e-11	7.0677e-09
Malic acid	1.4603	2.2221e-10	8.7772e-09
Fumaric acid	1.383	3.5883e-10	9.4491e-09
Aconitate	1.4654	7.0907e-08	1.235e-06
2-aminobutyric acid	1.2619	7.8167e-08	1.235e-06
Glutathione	0.26167	1.526e-07	2.0093e-06
Citric acid	1.4012	1.8841e-07	2.1264e-06
Argininosuccinic acid	1.4044	8.0989e-07	7.9976e-06
γ-Glutamylcysteine	0.38874	2.4983e-06	2.193e-05
N-Acetylaspartic acid	1.4012	5.9313e-06	4.6858e-05
Succinic acid	1.2442	9.4702e-06	6.8013e-05
Oxidized glutathione	0.53446	1.206e-05	7.9393e-05
S-adenosylhomocysteine	0.67941	2.2869e-05	0.00013898
Valine	0.78981	0.0001452	0.00081935
Isoleucine	0.8245	0.00018176	0.00095725
Aspartic acid	1.2697	0.00044392	0.0021918
Threonic acid	1.3235	0.00055436	0.0025761
Ornithine	0.80762	0.00067636	0.0029685
Oxoglutaric acid	1.2475	0.0008545	0.0035529
Pantothenic acid	1.0773	0.00099844	0.0037844
Choline	0.88625	0.001006	0.0037844
Leucine	0.85471	0.00139	0.0049616
Glycine	1.1806	0.0014445	0.0049616
Lactic acid	0.95114	0.001715	0.0056453
D gluconic acid sodium salt	1.1862	0.001793	0.005666
Phenylalanine	0.89058	0.0025434	0.0077046
Putrescine	1.2476	0.0026332	0.0077046
Glutamine	1.3081	0.0042679	0.012042
Methionine	0.90562	0.0048398	0.013184
Folic acid	0.84262	0.0055765	0.014685
Cytidine monophosphate	1.1084	0.0061877	0.015769
Tyrosine	0.89841	0.0077896	0.019231
Citrulline	0.84895	0.009764	0.023375
Tryptophan	0.89982	0.010347	0.02404
Gluconic acid	1.1258	0.013037	0.029427
Asparagine	1.2753	0.02567	0.05633
Arginine	0.87285	0.034574	0.073094
Deoxyadenosine monophosphate	1.077	0.035159	0.073094

2.6. RT-qPCR

RNA was extracted together with proteins using the NucleoSpin® RNA/Protein extraction kit. RNA quantification was performed using a Nanodrop® spectrophotometer (ND-1000). To eliminate residual DNA, samples were treated using DNase I Kits (sigma AMPD1). One μg of RNA was then reverse-transcribed into complementary DNA (cDNA) using Superscript II RT, random primers and RNasin® ribonuclease inhibitor (Promega N2511). All these steps were carried out following the manufacturer's instructions. For qPCR reaction, a mix was prepared for each sample containing 40 ng of cDNA, 2.5 μL of a mix of forward and reverse primers (final concentration for each primer: 1 μM), 12.5 μL of QuantiFast® SYBER® Green PCR Kit and q.s. 25 μL RNAse-free water. The reaction was performed on a Rotor Gene Q (Qiagen) using the following program: 5 min at 95 °C followed by 45 cycles of 10 s at 95 °C, 30 s at 60 °C. Acquisition was done in green. Fold-change was calculated ($2^{-\Delta\Delta Ct}$) and statistical analysis performed using paired t-test with Prism 5.0 software. The complete list of primers used is presented in Supplemental Table 1.

3. Results

Cell viability was not affected after 24 h and 48 h of treatment with 5 μM of tacrolimus. At 72 h, the MTS test showed a significant (p = 0.0003) but slight (5%) decrease in cell viability, while flow cytometry analysis did not show any difference (Fig. 1).

3.1. Intracellular metabolomics

Seventy-nine metabolites were detected by LC-MS/MS and heat-map analysis clearly discriminated the two conditions (controls or tacrolimus) (Fig. 2 A and Supplemental Table 2). PCA neatly separated the two experimental conditions too, with 47.6% of the variation being explained by the first component and 21.8% by the second (Fig. 2).

Univariate analysis (t-test) showed that 20 of these metabolites were significantly increased and 15 significantly decreased (p-value<0.05 and FDR<0.05) (Fig. 2B and Table 1). Most of these metabolites were amino acids, citric acid cycle intermediates, urea cycle intermediates and antioxidant reaction intermediates.

Enrichment pathway analysis of these 35 metabolites revealed that tacrolimus induces changes in the urea cycle, in the amino acid metabolism, in the citric acid cycle and in glutathione metabolism (Fig. 2 C).

3.2. Extracellular metabolomics

Fifty-nine metabolites were detected by LC-MS/MS and, as for intracellular metabolites, heat-map analysis clearly discriminated the control and tacrolimus-treated conditions (Fig. 3 A and Supplemental table 3). PCA also separated them neatly by means of the first two principal components, 30.3% of the variation being explained by the first and 16.5% by the second (Fig. 3B).

Out of the 59 metabolites detected in the extracellular medium, 17 were significantly impacted (p-value <0.05 and FDR<0.05) by tacrolimus exposure, including amino acids, citric acid cycle intermediates and purine and pyrimidine bases (Fig. 3 and Table 2). Enrichment pathway analysis confirmed that the pathways significantly impacted are those of the urea cycle, amino acid metabolism, pyrimidine and glutathione metabolism (Fig. 3 C).

3.3. Intracellular proteomics

A total of 846 proteins were identified and quantified among the 6 replicates (Supplemental table 4). Only proteins identified using more than 2 peptides were retained. Eleven proteins were found to be differentially expressed, all down-regulated (Fig. 4).

Two of these proteins are involved in anabolic processes (gluconeogenesis for PCK-1, the Phosphoenolpyruvate CarboxyKinase 1, and fatty acid synthesis for FASN, a Fatty Acid Synthase), and two others are subunits of the complex 1 involved in the mitochondrial membrane respiratory chain (NDUFA5, the NADH dehydrogenase [ubiquinone] 1 alpha subcomplex subunit 5, and NDUFV2, the NADH dehydrogenase [ubiquinone] flavoprotein 2). PCK-1 was the most down-regulated protein and was consistently down-regulated in the 6 independent experiments, with a mean delta of 0.42 corresponding to a 35% decrease (p < 0.0001).

3.4. Intracellular targeted transcriptomics

Downregulation of PCK-1 mRNA was confirmed by RT-qPCR (p = 0.0329). FBP1, a limiting enzyme in gluconeogenesis was also significantly downregulated (p = 0.0031), while FBP2, the other limiting enzyme in gluconeogenesis, was not significantly decreased (Fig. 5).

4. Discussion

This study of the acute off-target effects of a high concentration of tacrolimus on a porcine cell line (LLC-PK1) suggests that tacrolimus increases the oxidative stress, perturbs the cell energy metabolism and downregulates gluconeogenesis in proximal tubular cells.

As summarized in Fig. 6, metabolomics investigations clearly showed increased oxidative stress through a decrease of the total content of intracellular glutathione (i.e. glutathione, oxidized glutathione and

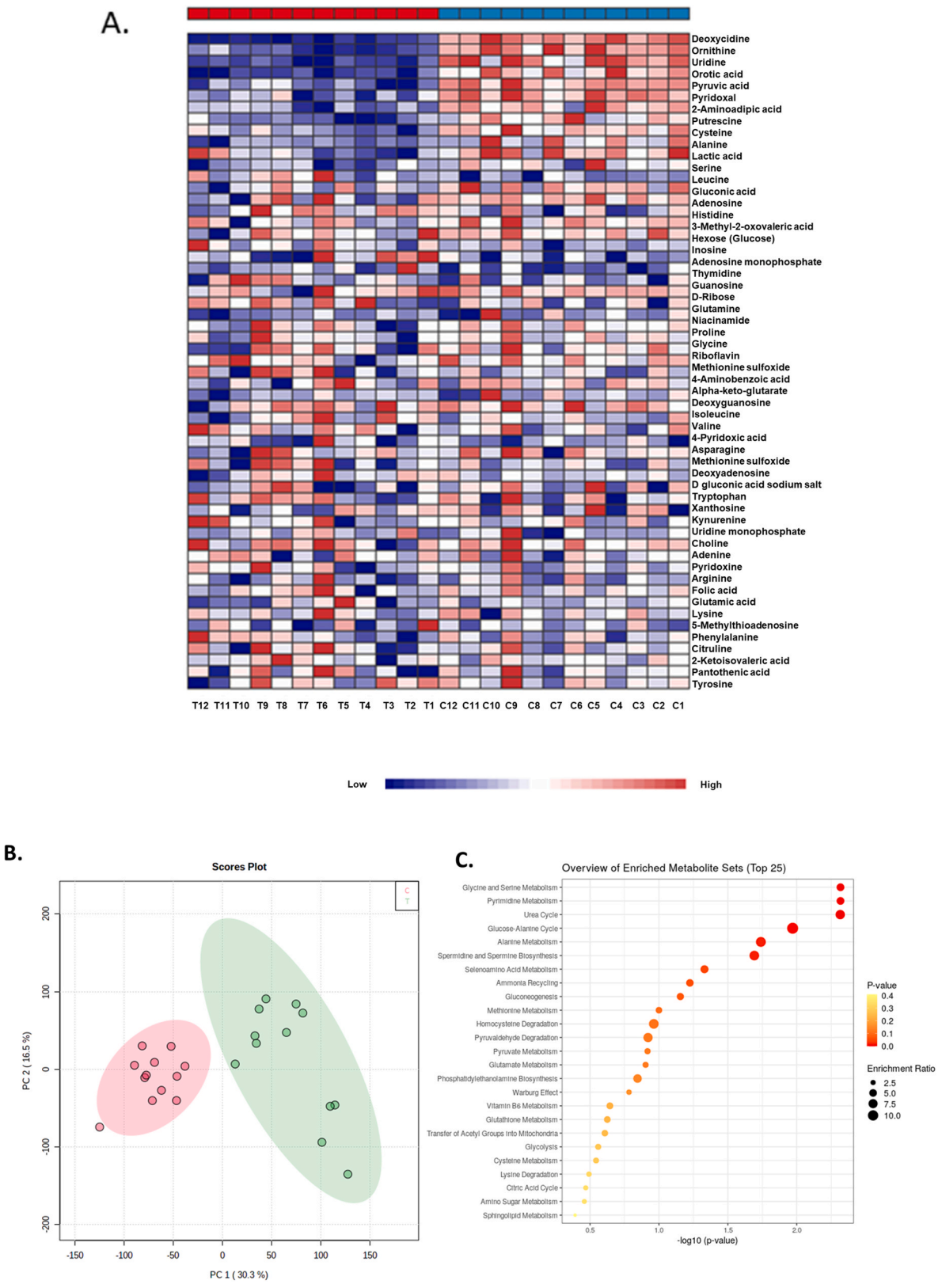

Fig. 3. .Multivariate exploration of extracellular metabolites variations after 24 h exposure to tacrolimus (n = 12). A. Heatmap clustering distinguishing control condition (C) and tacrolimus treated cells (T), based on all metabolites detected by LC-MS/MS analysis. B. PCA scores plot showing complete separation between groups (C) and (T) with principal component PC1 and PC2 describing 30.3% and 16.5% of the variations, respectively (0 (red circles): 0.5% ethanol (control); 1 (green circles): tacrolimus 5 μM for 24 h). C. Dot plot of pathway enrichment analysis based on extracellular concentrations of metabolites significantly modified in tacrolimus treated cells as compared to controls (Table 2).

Table 2
Fold-change of extracellular metabolites significantly influenced by tacrolimus (n = 12) (C.M.: culture medium, N.D: not detected, D: detected).

Metabolite	Fold-change	P-value (T-test)	FDR	Native C.M.	Interpretation
Deoxycytidine	0.36552	1.12E-15	6.47E-14	N.D	Secretion
Cytidine	0.38697	2.27E-12	6.57E-11	N.D	Secretion
Ornithine	0.64299	1.36E-10	2.63E-09	N.D	Secretion
Uridine	0.47507	2.41E-09	2.94E-08	N.D	Secretion
Orotic acid	0.4276	2.53E-09	2.94E-08	N.D	Secretion
Pyruvic acid	0.80938	6.15E-09	5.95E-08	D	Secretion
Pyridoxal	0.86522	2.81E-07	2.33E-06	D	Secretion
2-Aminoadipic acid	0.74831	1.88E-05	0.00013647	N.D	Secretion
Putrescine	0.72803	3.09E-05	0.000199	D	Secretion
Cystine	0.84703	5.47E-05	0.00031711	D	Uptake
Alanine	0.78346	0.0006475	0.003414	D	Secretion
Lactic acid	0.91772	0.0036161	0.017478	N.D	Secretion
Serine	0.87821	0.0088553	0.039508	D	Secretion
Leucine	1.0455	0.018112	0.075034	D	Uptake
Gluconic acid	0.88113	0.023577	0.091165	D	Uptake
Threonine	0.9359	0.028988	0.10508	D	Uptake

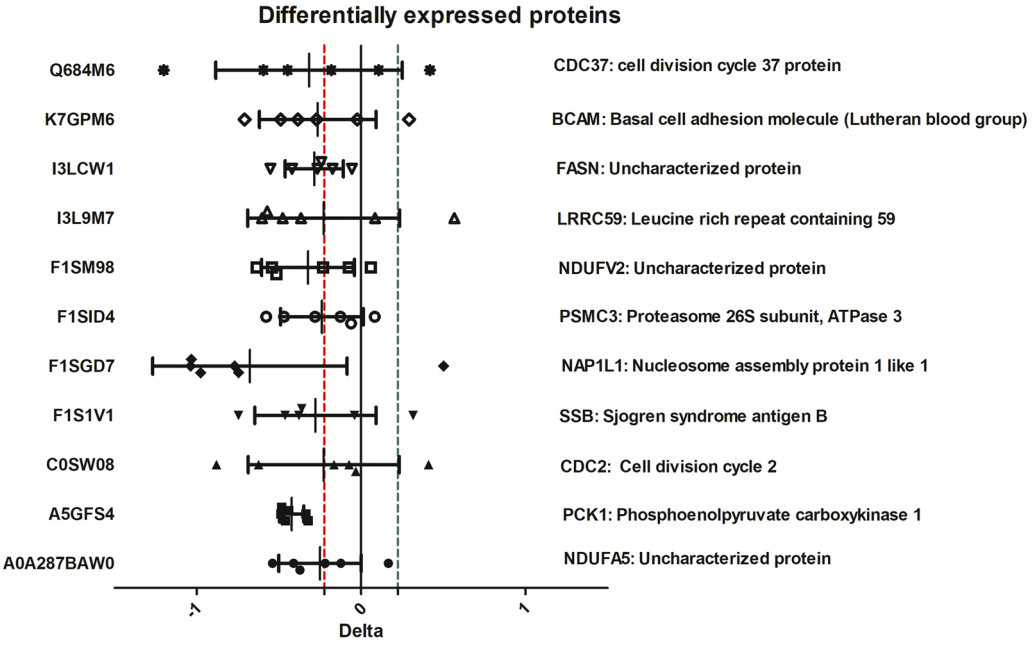

Fig. 4. Intracellular variations in proteins induced by tacrolimus. Intracellular concentrations of proteins modified after 24 h exposure to 5 μM of tacrolimus, as determined by SWATH proteomics analysis (n = 6 independent experiments). Proteins with a mean delta <ln(0.8) or >-ln(0.8) were regarded as differentially expressed.

γ-glutamyl-cysteine) in tacrolimus-treated cells. Moreover, the lower extracellular quantity of cystine in the culture medium (Fig. 3 A, Table 2) suggests an increased uptake of this source of cysteine for glutathione synthesis. Furthermore, increased consumption of folate, known for its free-radical scavenging property, by tacrolimus-treated cells (Table 1) also points towards oxidative stress. Actually, folate metabolism is a major source of NADPH, a cofactor of glutathione reductase in charge of the regeneration of glutathione from oxidized glutathione [8]. These results are consistent with previous observations of tacrolimus toxicity mediated by oxidative stress [18,32] and they validate our experimental setting aimed to detect off-target effects of tacrolimus.

Besides, tacrolimus altered the TCA cycle, as clearly shown by intracellular increase of TCA cycle intermediates (Table 1, Fig. 3 and 8). This alteration can be linked with various intracellular events that can induce an accumulation or an increased synthesis of TCA intermediates. Moreover, lactic acid was less excreted and its intracellular concentration decreased (Table 2), which is in favor of an impaired citric acid flux. Our findings suggest possible origins to these TCA cycle perturbations. Similar to folic acid metabolism, the citric acid cycle is a major source of NADPH, which is generated by isocitrate dehydrogenase and malic enzyme and is essential to reduce oxidative stress. Thus, the increase of the citric acid cycle intermediates may be considered as a response to oxidative stress. Reciprocally, oxidative stress can reduce the activity of some citric acid enzymes like aconitase, oxoglutarate dehydrogenase and succinic dehydrogenase, which may also result in citric acid cycle intermediate accumulation [26]. Our proteomics investigations showed differently expressed proteins, with PCK-1 being the most down-regulated (Fig. 4). PCK-1 is a limiting enzyme in the gluconeogenesis process that converts oxaloacetate to phosphoenolpyruvate. Interestingly, decreased PCK-1 activity could cause an accumulation of TCA intermediates by limiting oxaloacetate transformation. For instance, PCK-1 -/- mice showed a tenfold increase in malate level in the liver as compared to controls [12]. In addition, this down-regulation of PCK-1 was also found in a human hepatic cell line, in primary cultured human β-pancreatic cells and in the liver of mice exposed to tacrolimus [14,20]. At the kidney level, a study conducted in rats treated with tacrolimus showed a downregulation of PCK-1 mRNA [23]. Given the

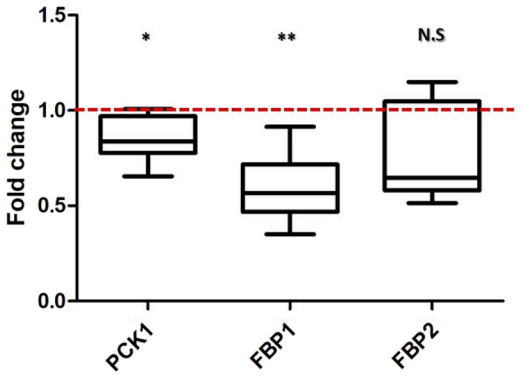

Fig. 5. Effect of tacrolimus exposure on the mRNA levels of PCK1, FBP1 and FBP2 in proximal tubular cells. Fold-change of PCK-1, FBP1 and FBP2 mRNAs in cells exposed to 5 μM tacrolimus (TAC) with respect to controls (C, exposed to 0.5% ethanol). Targeted gene mRNA signals were normalized to the signal of GAPDH mRNA, as housekeeping gene. * $p < 0.05$; * * $p < 0.01$ by student *t*-test (n = 6 independent experiments).

difficulties encountered to find antibodies against porcine proteins in general, and against Sus scrofa PCK-1 in particular, and also because trying to confirm high-resolution mass spectrometry identification and determination of proteins with Western blot assays seems anachronic, we chose to strengthen our proteomics results by measuring the expression of the corresponding mRNAs. RT-qPCR confirmed that PCK-1 mRNA was down-regulated when cells were exposed to tacrolimus (Fig. 5), in line with the above-mentioned studies and our proteomics findings.

TCA cycle impairment can have other origins. One of them is increased glycolysis, essential to produce NADPH that plays an important role in reducing oxidative stress. Another is the stress of the endoplasmic reticulum, known to be implicated in tacrolimus nephrotoxicity and that can increase the citric acid cycle flux mediated by the redox metabolites [9]. Unfortunately, our rather large, but still targeted metabolomics method, may have hampered the identification of key metabolites. Fluxomic approaches could enhance the characterization of tacrolimus-induced TCA cycle perturbations. Monitoring TCA intermediates and glycolysis products during tacrolimus treatment using labelled metabolites could help to determine whether tacrolimus causes an accumulation of TCA intermediates or an increase of the citric acid cycle flux [21].

Metabolites belonging to the urea cycle were found to be impacted by tacrolimus (Fig. 6). Although metabolomics pathway analysis also pointed towards an impact on the urea cycle, proximal tubular cells do not express key urea cycle enzymes, e.g. ornithine transcarbamylase [16]. Therefore, tacrolimus disrupted the arginine metabolism. Aspartate, arginosuccinate and fumarate levels were increased in tacrolimus-treated cells, while the levels of arginine, citrulline and ornithine were decreased. They released less ornithine in the medium. Intracellular putrescine, a product of ornithine, increased and its excretion decreased. This may imply a perturbation of the transporter-dependent secretion of putrescine, alone or associated with a potential increase in putrescine synthesis. Interestingly, the accumulation of putrescine can lead to cytotoxicity [25,28].

In order to investigate if tacrolimus affects only PCK-1 or impacts the whole gluconeogenesis process, mRNA expression of FBP1 and FBP2, two other limiting enzymes in this process, was investigated. Results show that tacrolimus significantly down-regulates FBP1, and probably FBP2 although it did not reach statistical significance (Fig. 5). This suggests that tacrolimus affects gluconeogenesis at large and reduces glucose synthesis. A study in C57BL/6 mice showed that glycemia after overnight fasting was lower and insulin higher after 2 weeks of treatment with 0.5 or 2 mg/kg/day tacrolimus, as compared to controls, confirming that tacrolimus affects gluconeogenesis [20]. Moreover, the same study suggested that tacrolimus increased insulin resistance based on glucose tolerance tests, showing higher insulin AUC at the two tacrolimus doses, and higher glucose concentration peak and AUC at the higher dose. It suggests that tacrolimus diabetogenic effect is mostly mediated by its impact on insulin secretion and activity, rather than on glucose catabolism [13]. Our hypothesis here is that tacrolimus effect on tubular cell gluconeogenesis may have more local than systemic consequences. Actually, decreased renal glucogenesis has recently been identified as a hallmark of chronic kidney disease [27]. In this study, the authors provided compelling evidence that gluconeogenesis downregulation was associated with: (i) decreased systemic lactate clearance (the main substrate for gluconeogenesis in the kidney is lactate); (ii) CKD progression in retrospective human studies; and (iii) faster histologic progression of kidney disease in kidney allograft biopsies [27]. They also showed that PCK-1, FBP1 as well as other gluconeogenic enzymes (PC and G6PC) were downregulated in CKD, in a stage-dependent manner.

PCK-1 downregulation can impact the acid-base balance. In case of acidosis, PCK-1 is upregulated in proximal tubular cells and increase the transformation of oxaloacetate to phosphoenolpyruvate and HCO_3- [1,7]. The latter is released in the blood stream to regulate the acid-base disorder. Tacrolimus favored faster (2 days) systemic acidosis when metabolic acidosis was induced with ammonium chloride in a murine model, whereas acidosis was comparable in mice with or without tacrolimus after chronic exposure to ammonium chloride (7 days) [22]. This observation was partially explained by alterations of renal acid-base transport proteins. PCK-1 downregulation by tacrolimus is a complementary explanation, in as much as PCK-1 is normally upregulated during intracellular acidosis induced by hypokalemia in vitro [11]. Actually, tacrolimus-dependent downregulation of PCK-1 can impact intracellular pH regulation and induce direct toxicity on proximal tubular cells.

All of the metabolomic and proteomic variations described above support tacrolimus-dependent dysregulation of the energy metabolism in tubular proximal cells. They recapitulate several of the proximal tubular cell dysregulations found in CKD [27] and point towards decreased gluconeogenesis as a potential pathway of tacrolimus toxicity. In addition, PCK-1 downregulation may affect the local acid-base balance.

The tacrolimus concentration used in this study (5 μM, equivalent to 4 μg/L) was about 1000 times higher than trough tacrolimus whole blood concentrations found in treated patients (typically 4–15 ng/ml). However, this concentration did not induce any cytotoxic effect after 24 h or even 48 h incubation (and only a mild effect on cell viability after 72 h) and it is at the lower end of the concentrations previously used to investigate tacrolimus nephrotoxicity on different cell lines in vitro, including LLCPK1, HEK293 or HK-2, which was up to 80 μM for periods of time ranging between 6 h and 48 h [10,17–19,29,32,4]. Interestingly, toxicity findings made at these relatively high concentrations could be validated in animal models of chronic tacrolimus nephrotoxicity [19,29]. This suggests that our results, obtained at intermediate concentrations, may raise pertinent hypotheses regarding tacrolimus toxicity pathways. Because tacrolimus nephrotoxicity (apart from its vasoconstrictive properties) is a delayed and chronic process, its in vitro exploration would ideally require a very long incubation time, but this is hardly feasible. There is no example in the literature we know of that employed a different strategy than using high concentrations of tacrolimus for short time-periods, and even “chronic toxicity” in vitro studies did not last more than a few days (maximum of 14 days in a rather old study on human renal proximal tubule cells) [3]. The strategy employed here should be regarded as a pharmacological investigation of the off-target effects of tacrolimus on tubular cells. This requires saturating FKBP12 and the other 16 FKBPs [2] that all have an FK-506 binding domain [15], and favoring tacrolimus binding to less affine targets. Finally, the variations reported here were observed at or after 24 h incubation and a kinetics study might allow better understanding

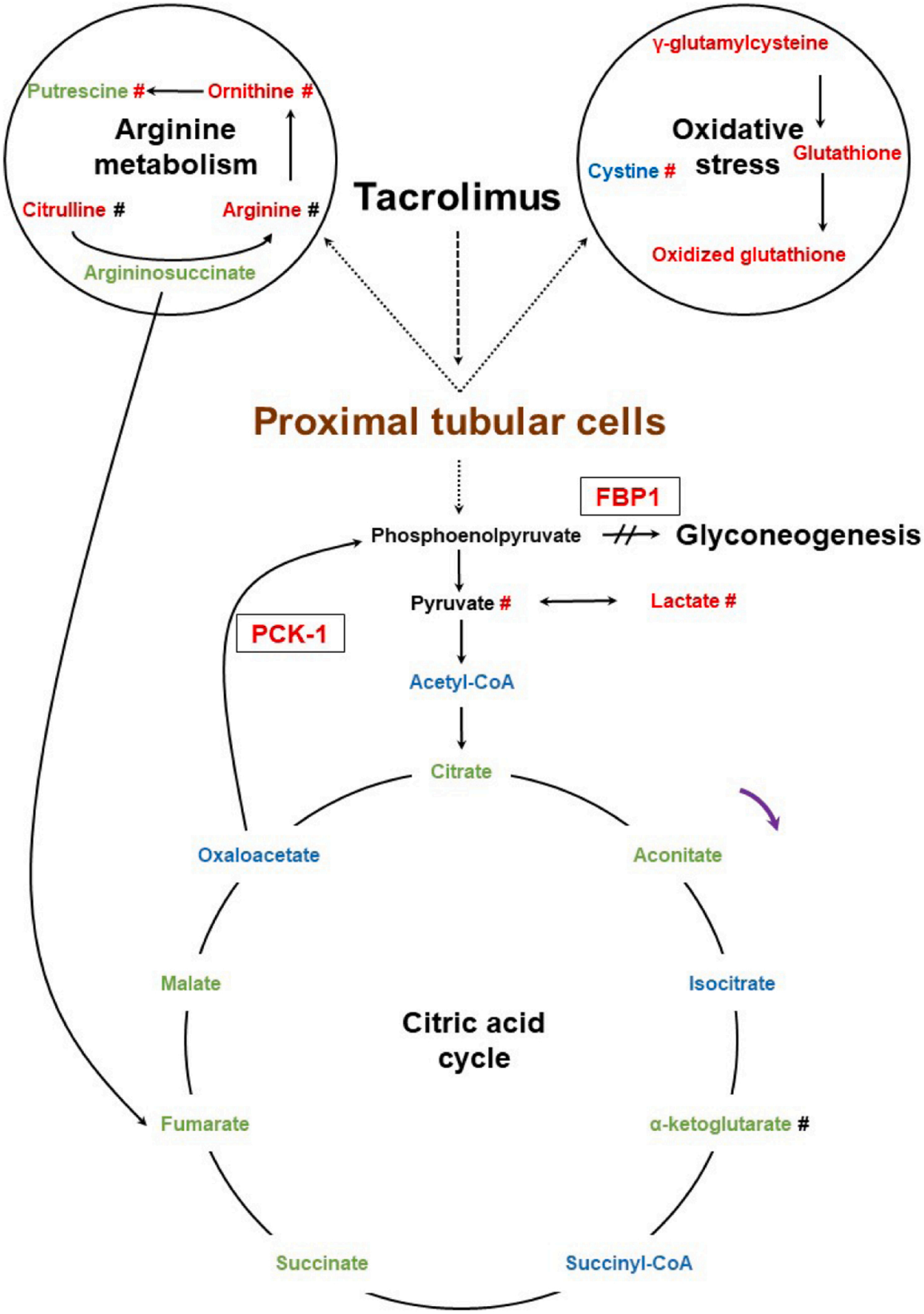

Fig. 6. Main pathways modulated by tacrolimus. Intracellular (name) and extracellular (marked with #) metabolites and intracellular proteins (in black boxes) are presented. Decreased metabolites are presented in green, increased metabolites in red, metabolites normally expressed in black and those not detected in blue. Downregulated proteins are presented in red. Purple arrows show cycle directions.

of tacrolimus underlying mechanisms.

In conclusion, this in vitro multi-omics study shows that tacrolimus can induce oxidative stress and alterations in the energy and glucose metabolisms in a proximal tubular cell line, particularly gluconeogenesis which is a hallmark of chronic kidney diseases. Whether these short-term modifications are actually implicated in tacrolimus nephrotoxicity must be further investigated in a chronic toxicity setting.

Funding

This research did not receive any specific grant from funding agencies in the public, commercial, or not-for-profit sectors.

Author Contributions

HA, QF, ME and PM participated in the research design. HA conducted the experiments. FLS, EM and HA contributed to the experiments. HA, QF and CCB performed data analysis. All authors contributed to the writing of the manuscript.

CRediT authorship contribution statement

Hassan Aouad: Methodology, Investigation, Data Curation, Writing - original draft preparation; **Quentin Faucher**: Methodology, Investigation, Writing - original draft preparation; **François-Ludovic Sauvage**: Methodology, Investigation, Writing - original draft preparation; **Emilie Pinault**: Methodology, Investigation, Writing - original draft preparation; **Claire-Cécile Barrot**: Software, Formal analysis; **Hélène Arnion**: Methodology, Investigation, Validation; **Marie Essig:** Conceptualization, Supervision, Writing – Review and Editing; **Pierre Marquet:** Conceptualization, Supervision, Writing – Review and Editing.

Declaration of Competing Interest

Pierre Marquet declares that he has received honoraria from Astellas, Chiesi and Sandoz over the last three years. The other authors declare that they have no commercial or financial relationships that could be construed as a potential conflict of interest.

Data Availability

Data will be made available on request.

Acknowledgments

The authors thank Jean-Sebastien Bernard for helping with the experiments.

Appendix A. Supporting information

Supplementary data associated with this article can be found in the online version at doi:10.1016/j.phrs.2023.106794.

References

[1] G.A. Alleyne, G.H. Scullard, Renal metabolic response to acid base changes. I. Enzymatic control of ammoniagenesis in the rat, J. Clin. Invest 48 (1969) 364–370, https://doi.org/10.1172/JCI105993.

[2] S. Annett, G. Moore, T. Robson, FK506 binding proteins and inflammation related signalling pathways; basic biology, current status and future prospects for pharmacological intervention, Pharmacol. Ther. 215 (2020), 107623, https://doi.org/10.1016/j.pharmthera.2020.107623.

[3] M.M. Atcherson, A.L. Trifillis, Cytotoxic effects of FK506 on human renal proximal tubule cells in culture, Vitr. Cell. Dev. Biol. Anim. 30A (1994) 562–567, https://doi.org/10.1007/BF02631253.

[4] J. Bennett, H. Cassidy, C. Slattery, M.P. Ryan, T. McMorrow, Tacrolimus modulates TGF-β signaling to induce epithelial-mesenchymal transition in human renal proximal tubule epithelial cells, J. Clin. Med 5 (2016) 50, https://doi.org/10.3390/jcm5050050.

[5] Brattström Böttiger, S.äwe Tydén, Groth, Tacrolimus whole blood concentrations correlate closely to side-effects in renal transplant recipients, Br. J. Clin. Pharm. 48 (1999) 445–448, https://doi.org/10.1046/j.1365-2125.1999.00007.x.

[6] M. Brunet, T. van Gelder, A. Åsberg, V. Haufroid, D.A. Hesselink, L. Langman, F. Lemaitre, P. Marquet, C. Seger, M. Shipkova, A. Vinks, P. Wallemacq, E. Wieland, J.B. Woillard, M.J. Barten, K. Budde, H. Colom, M.-T. Dieterlen, L. Elens, K.L. Johnson-Davis, P.K. Kunicki, I. MacPhee, S. Masuda, B.S. Mathew, O. Millán, T. Mizuno, D.-J.A.R. Moes, C. Monchaud, O. Noceti, T. Pawinski, N. Picard, R. van Schaik, C. Sommerer, N.T. Vethe, B. de Winter, U. Christians, S. Bergan, Therapeutic drug monitoring of tacrolimus-personalized therapy: second consensus report, Ther. Drug Monit. 41 (2019) 261–307, https://doi.org/10.1097/FTD.0000000000000640.

[7] N.P. Curthoys, G. Gstraunthaler, Mechanism of increased renal gene expression during metabolic acidosis, Am. J. Physiol. Ren. Physiol. 281 (2001) F381–390, https://doi.org/10.1152/ajprenal.2001.281.3.F381.

[8] J. Fan, J. Ye, J.J. Kamphorst, T. Shlomi, C.B. Thompson, J.D. Rabinowitz, Quantitative flux analysis reveals folate-dependent NADPH production, Nature 510 (2014) 298–302, https://doi.org/10.1038/nature13236.

[9] E.R. Gansemer, K.S. McCommis, M. Martino, A.Q. King-McAlpin, M.J. Potthoff, B. N. Finck, E.B. Taylor, D.T. Rutkowski, NADPH and glutathione redox link TCA cycle activity to endoplasmic reticulum homeostasis, iScience 23 (2020), 101116, https://doi.org/10.1016/j.isci.2020.101116.

[10] C. González-Guerrero, C. Ocaña-Salceda, S. Berzal, S. Carrasco, B. Fernández-Fernández, P. Cannata-Ortiz, J. Egido, A. Ortiz, A.M. Ramos, Calcineurin inhibitors recruit protein kinases JAK2 and JNK, TLR signaling and the UPR to activate NF-κB-mediated inflammatory responses in kidney tubular cells, Toxicol. Appl. Pharmacol. 272 (2013) 825–841, https://doi.org/10.1016/j.taap.2013.08.011.

[11] G. Gstraunthaler, T. Holcomb, E. Feifel, W. Liu, N. Spitaler, N.P. Curthoys, Differential expression and acid-base regulation of glutaminase mRNAs in gluconeogenic LLC-PK1-FBPase+ cells, Am. J. Physiol. -Ren. Physiol. 278 (2000) F227–F237, https://doi.org/10.1152/ajprenal.2000.278.2.F227.

[12] P. Hakimi, M.T. Johnson, J. Yang, D.F. Lepage, R.A. Conlon, S.C. Kalhan, L. Reshef, S.M. Tilghman, R.W. Hanson, Phosphoenolpyruvate carboxykinase and the critical role of cataplerosis in the control of hepatic metabolism, Nutr. Metab. 2 (2005) 33, https://doi.org/10.1186/1743-7075-2-33.

[13] R.M. Jindal, R.A. Sidner, M.L. Milgrom, Post-transplant diabetes mellitus, role Immunosuppr. Drug Saf. 16 (1997) 242–257, https://doi.org/10.2165/00002018-199716040-00002.

[14] J. Kolic, L. Beet, P. Overby, H.H. Cen, E. Panzhinskiy, D.R. Ure, J.L. Cross, R. B. Huizinga, J.D. Johnson, Differential effects of voclosporin and tacrolimus on insulin secretion from human islets, Endocrinology (2020) 161, https://doi.org/10.1210/endocr/bqaa162.

[15] J.M. Kolos, A.M. Voll, M. Bauder, F. Hausch, FKBP ligands—where we are and where to go? Front. Pharmacol. (2018) 9.

[16] O. Levillain, A. Hus-Citharel, S. Garvi, S. Peyrol, I. Reymond, M. Mutin, F. Morel, Ornithine metabolism in male and female rat kidney: mitochondrial expression of ornithine aminotransferase and arginase II, Am. J. Physiol. Ren. Physiol. 286 (2004) F727–738, https://doi.org/10.1152/ajprenal.00315.2003.

[17] S.W. Lim, L. Jin, K. Luo, J. Jin, Y.J. Shin, S.Y. Hong, C.W. Yang, Klotho enhances FoxO3-mediated manganese superoxide dismutase expression by negatively regulating PI3K/AKT pathway during tacrolimus-induced oxidative stress, Cell Death Dis. 8 (2017), e2972, https://doi.org/10.1038/cddis.2017.365.

[18] S.W. Lim, Y.J. Shin, K. Luo, Y. Quan, S. Cui, E.J. Ko, B.H. Chung, C.W. Yang, Ginseng increases Klotho expression by FoxO3-mediated manganese superoxide dismutase in a mouse model of tacrolimus-induced renal injury, Aging 11 (2019) 5548–5569, https://doi.org/10.18632/aging.102137.

[19] S.W. Lim, Y.J. Shin, K. Luo, Y. Quan, E.J. Ko, B.H. Chung, C.W. Yang, Effect of Klotho on autophagy clearance in tacrolimus-induced renal injury, FASEB J. 33 (2019) 2694–2706, https://doi.org/10.1096/fj.201800751R.

[20] Q. Ling, H. Huang, Y. Han, C. Zhang, X. Zhang, K. Chen, L. Wu, R. Tang, Z. Zheng, S. Zheng, L. Li, B. Wang, The tacrolimus-induced glucose homeostasis imbalance in terms of the liver: From bench to bedside, Am. J. Transpl. 20 (2020) 701–713, https://doi.org/10.1111/ajt.15665.

[21] P.K. Lorkiewicz, A.A. Gibb, B.R. Rood, L. He, Y. Zheng, B.F. Clem, X. Zhang, B. G. Hill, Integration of flux measurements and pharmacological controls to optimize stable isotope-resolved metabolomics workflows and interpretation, Sci. Rep. 9 (2019) 13705, https://doi.org/10.1038/s41598-019-50183-3.

[22] N. Mohebbi, M. Mihailova, C.A. Wagner, The calcineurin inhibitor FK506 (tacrolimus) is associated with transient metabolic acidosis and altered expression of renal acid-base transport proteins, Am. J. Physiol. -Ren. Physiol. 297 (2009) F499–F509, https://doi.org/10.1152/ajprenal.90489.2008.

[23] S.M. Morris, D. Kepka-Lenhart, N.P. Curthoys, R.L. McGill, R.J. Marcus, S. Adler, Disruption of renal function and gene expression by FK 506 and cyclosporine, Transplant. Proc. 23 (1991) 3116–3118.

[24] P.F. Secker, N. Schlichenmaier, M. Beilmann, U. Deschl, D.R. Dietrich, Functional transepithelial transport measurements to detect nephrotoxicity in vitro using the RPTEC/TERT1 cell line, Arch. Toxicol. 93 (2019) 1965–1978, https://doi.org/10.1007/s00204-019-02469-8.

[25] E.M. Tome, M.S. Fiser, M.C. Payne, W.E. Gerner, Excess putrescine accumulation inhibits the formation of modified eukaryotic initiation factor 5A (eIF-5A) and induces apoptosis, Biochem. J. 328 (1997) 847–854, https://doi.org/10.1042/bj3280847.

[26] L. Tretter, V. Adam-Vizi, Alpha-ketoglutarate dehydrogenase: a target and generator of oxidative stress, Philos. Trans. R. Soc. B Biol. Sci. 360 (2005) 2335–2345, https://doi.org/10.1098/rstb.2005.1764.

[27] T. Verissimo, A. Faivre, A. Rinaldi, M. Lindenmeyer, V. Delitsikou, C. Veyrat-Durebex, C. Heckenmeyer, M. Fernandez, L. Berchtold, D. Dalga, C. Cohen, M. Naesens, S.E. Ricksten, P.Y. Martin, J. Pugin, F. Merlier, K. Haupt, J. M. Rutkowski, S. Moll, P.E. Cippà, D. Legouis, S. de Seigneux, Decreased renal gluconeogenesis is a hallmark of chronic kidney disease, J. Am. Soc. Nephrol. 33 (2022) 810–827.

[28] X. Xie, M.E. Tome, E.W. Gerner, Loss of intracellular putrescine pool-size regulation induces apoptosis, Exp. Cell Res. 230 (1997) 386–392, https://doi.org/10.1006/excr.1996.3442.

[29] J.H. Yu, S.W. Lim, K. Luo, S. Cui, Y. Quan, Y.J. Shin, K.E. Lee, H.L. Kim, E.J. Ko, B. H. Chung, J.H. Kim, S.J. Chung, C.W. Yang, Coenzyme Q10 alleviates tacrolimus-induced mitochondrial dysfunction in kidney, FASEB J. 33 (2019) 12288–12298, https://doi.org/10.1096/fj.201900386RR.

[30] M. Yuan, S.B. Breitkopf, X. Yang, J.M. Asara, A positive/negative ion–switching, targeted mass spectrometry–based metabolomics platform for bodily fluids, cells, and fresh and fixed tissue, Nat. Protoc. 7 (2012) 872–881, https://doi.org/10.1038/nprot.2012.024.

[31] H. Zheng, H. Zhang, C. Zhu, H. Li, S. Cui, Jian Jin, S. Piao, Y. Jiang, M. Xuan, Ji-zhe Jin, Y. Jin, J. Lee, B. Chung, B. Choi, C. Yang, C. Li, L -C arnitine protects against tacrolimus-induced renal injury by attenuating programmed cell death via PI3K/AKT/PTEN signaling, Acta Pharmacol. Sin. (2020) 1–11, https://doi.org/10.1038/s41401-020-0449-8.

[32] X. Zhou, G. Yang, C.A. Davis, S.Q. Doi, P. Hirszel, C.S. Wingo, A. Agarwal, Hydrogen peroxide mediates FK506-induced cytotoxicity in renal cells, Kidney Int 65 (2004) 139–147, https://doi.org/10.1111/j.1523-1755.2004.00380.x.